Matrix Isolation Infrared and Ab- Initio Study of Propargyl alcohol and Methyl amine Complexes

Gargi Satishraj Jagdale

A dissertation submitted for the partial fulfillment of BS-MS dual degree in Science

Indian Institute of Science Education and Research, Mohali
April 2015

Certificate of Examination

This is to certify that the dissertation titled "**Matrix Isolation Infrared and Ab-initio Study of Propargyl alcohol and Methyl amine Complexes**" submitted by Ms. Gargi Satishraj Jagdale (Reg. No.: MS10032) for the partial fulfillment of BS-MS dual degree programme of the Institute has been examined by the thesis committee duly appointed by the Institute. The committee finds the work done by the candidate satisfactory and recommends that the report be accepted.

Dr. P. Balanarayan	**Dr. Sugumar Venkataramani**	**Dr. K.S. Viswanathan**
		(Supervisor)

Dated: April 24, 2015

Declaration

The work presented in this dissertation has been carried out by me under the guidance of Prof. K. S. Viswanathan at the Indian Institute of Science Education and Research (IISER) Mohali.

This work has not been submitted in part or in full for a degree, a diploma, or a fellowship to any other university or institute. Whenever contributions of others are involved, every effort is made to indicate this clearly, with due acknowledgement of collaborative research and discussions. This thesis is a bonafide record of original work done by me and all sources listed within have been detailed in the bibliography.

Gargi Jagdale

Dated: April 24, 2015

In my capacity as the supervisor of the candidates' project work, I certify that the above statements by the candidate are true to the best of my knowledge.

Prof. K. S. Viswanathan

(Supervisor)

Acknowledgement

I express the deepest appreciation and gratitude to my thesis supervisor, Prof. K. S. Viswanathan, who carries a very enthusiastic attitude towards research. His dedication towards work and involvement is very inspiring. His valuable advices, discussions and constant encouragement gave me a very good learning experience.

I sincerely thank my Master’s thesis committee members, Dr. P. Balanarayan and Dr. Sugumar Venkataramani for their valuable suggestions and comments during the committee meeting.

I am thankful to my lab members Ginny, Kanupriya, Jyoti, Pankaj, Akshay and Piyush who accompanied me throughout the research work. The discussions with them helped me gain a lot of information in a playful way.

I take this opportunity to thank my friends, classmates who where always there for me in the entire 5 years duration of my BS-MS integrated course. I am also thankful to the neighboring lab members for maintaining a friendly atmosphere in the work place.

I express my sincere gratitude to my family for their constant support and encouragement throughout the course of study.

I would like to acknowledge the Department of Science and Technology (DST), India for providing the INSPIRE fellowship.

List of Figures

List of Tables

List of Abbreviations

ISM	Interstellar Medium
DNA	Deoxyribonucleic acid
HF	Hartree-Fock
MP2	Møller–Plesset second order perturbation theory
CCSD	Coupled-cluster singles doubles
DFT	Density Function Theory
B3LYP	Becke-three parameter-Lee-Yang-Parr non-local exchange functional
M06	Minnesota functional
PAH	Polycyclic aromatic hydrocarbons
PA	Propargyl alcohol
MA	Methyl amine
AIM	Atoms- in- molecule
FT-IR	Fourier Transform Infrared
ZPE	Zero Point Energy
BSSE	Basis set superposition error

Contents

Chapter 1 Introduction

Chapter 2 Experimental and Computational Procedure

Chapter 3 Study of Propargyl alcohol complexes with Methyl amine

Abstract

The interstellar medium is filled with very cold and dense molecular clouds. These icy clouds contribute to the structure and evolution of the interstellar medium. Among various molecular clouds, the ones containing hydrogen bonds have special importance. Propargyl alcohol and methyl amine are two such molecules. Propargyl alcohol further gains importance because of the known propargyl radical pathway for benzene formation.

Matrix isolation infrared spectroscopy corroborated with quantum chemical calculations serves as a powerful tool to study weak interactions in a system. This technique is characterized to give very sharp spectral features, making it possible to identify and study various conformations and complexes formed by weak interactions.

In this thesis, propargyl alcohol with methyl amine system has been explored experimentally and supported with computational calculations. Calculations were performed at B3LYP, MP2 and M06-2x levels of theory using the 6-311++G(d,p) basis set to obtain optimized structures, stabilization energies and vibrational frequencies of the intuitive structures. The calculated results were used to support the experimental results. The O-H…N and the C≡C-H…N structures which are global and local minima respectively were identified in the matrix.

Methyl amine and water system was also studied in a similar manner. 1:1 and 1:2 adducts of methyl amine with water were identified in the matrix.

Chapter 1: Introduction

The voids between the stars of our and other galaxies are filled with tenuous material. These voids are called interstellar medium (ISM). The ISM is composed of several types of clouds (Spaans & Ehrenfreund 1999). Dense and very cold molecular clouds harbor icy particles which play a crucial role in the structure and evolution of the ISM. Thus their identification and study in the astrochemical environment is crucial to understand and trace back the events that happened, are happening or can possibly happen in the space. Among all, the molecular solids composed of chemical systems containing hydrogen bonds are of special importance.

1.1 Hydrogen Bonding

Hydrogen bond is the attractive force between the hydrogen attached to an electronegative atom of a molecule and an electronegative atom/site of another molecule. It is usually stronger than normal dipole forces between molecules. Hydrogen bonding is not nearly as strong as normal covalent bonds within a molecule; it is only about 1/10 as strong. This interaction is still strong enough to have many important ramifications on the properties of the molecules involved. The hydrogen bond is represented as X-H$^{\cdots}$Y where X is an atom with electro-negativity higher than that of hydrogen (eg- C, O, N,F) and Y can be a π or σ electron donor site. The π cloud can interact with X-H group (X=C, N, or O) to form a hydrogen bond; which is generally weaker than the conventional one. The π electron system acting as an electron donor was first proposed by Dewar in 1944.[1.]
It has been observed in studies that formation of the hydrogen bond, i.e. H$^{\cdots}$Y results in the weakening of the covalent bond X-H. As a result, the X-H stretching frequency decreases. [2.] This red shift is one of the most important characteristics of H-bonding interactions. Another characteristic feature is the considerable change in intensity of the spectral band corresponding to X-H stretch, indicating a non-negligible electron density transfer from proton acceptor to donor.

1.2 Study of Hydrogen Bond

Hydrogen bonds have played an incredibly important role in the history of structural biology and more. Both the structures of DNA and proteins (α-helices and β-sheets) were predicted based largely on the hydrogen bonds formed in these structures. Hydrogen bonding gives the molecule specific structure and directionality. For example in DNA, the two strands are held in particular order by a regular base-pairing between the strands. Adenine is paired to Thymine with two H-bonds and Guanine is paired to Cytosine with three H-bonds (Figure1a). Thousands of such hydrogen bonds are present in a DNA molecule; contributing greatly to the stability of the double helix structure. Van der Waals and hydrophobic interactions between the stacked adjacent pairs further stabilizes the DNA structure.

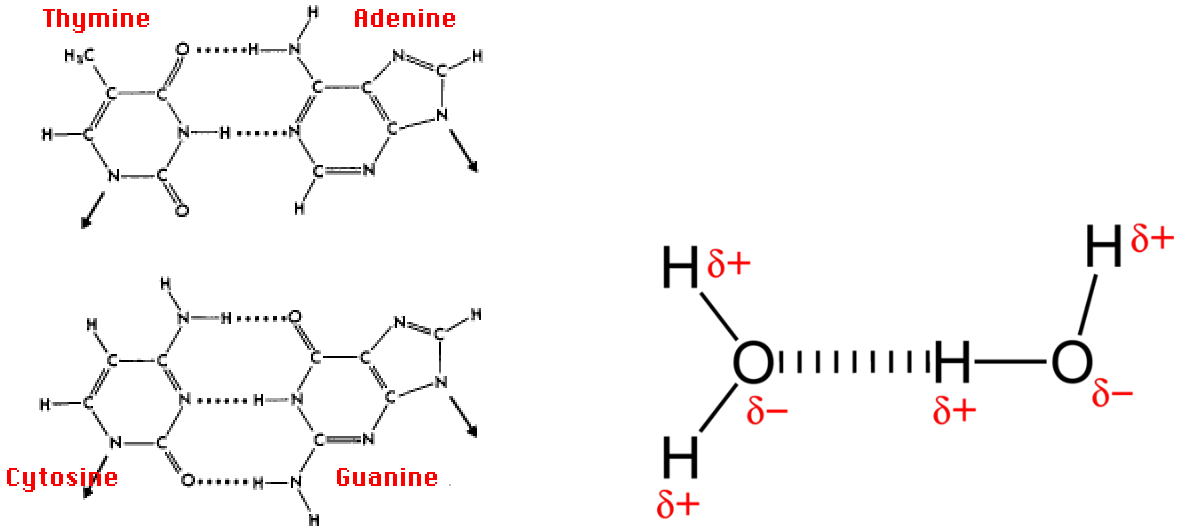

Figure 1: a) base-pairing in DNA **b) hydrogen bonding in water**

Hydrogen bonding is also seen in simple molecule like water (Figure 1b). Specific heat capacity and thus boiling point of water are governed by this hydrogen bonding. The average heat emitted by the sun is not enough to break those bonds preventing boiling of water; which is why the water bodies on earth can hold water. H-bonds also ensure the reduction of temperature extremes in large bodies of water. So, understanding hydrogen bonds is clearly important. But these bonds are surprisingly complex and are not completely understood till every last detail. Even in simple molecules of water, we see that one molecule acts as a proton donor while the other one as proton acceptor. It can also happen that the same oxygen is donating its hydrogen to a neighboring molecule while accepting another one from another neighboring molecule. This makes one molecule of water possess multiple hydrogen bonding sites.

There have been numerous experimental as well as theoretical studies on H- bonding. Nuclear magnetic resonance (NMR) and infrared (IR) spectroscopy are used widely to analyze the hydrogen bonding interactions in many systems. Spectroscopic information obtained from these techniques is used to probe the H-bonding interactions. Theoretical methods are also being used to analyze these interactions. Semi-empirical molecular orbital methods like Hartree-Fock, others like Møller–Plesset (MP2), coupled-cluster singles doubles (CCSD) and density functional theory (DFT) are widely used to investigate H-bonding interactions. The results calculated for bond length, bond angle, electronic properties, interaction energy and vibrational spectra depend on the basis set used in the calculation. These calculations, sometimes combined with some corrections are used to estimate geometrical parameters and energetics of the H-bonded systems.

1.3 Motivation of Present Work

Polycyclic aromatic hydrocarbons (PAHs), PAH cations and PAH clusters have been identified in planetary atmospheres, in the interstellar medium and in the envelopes of carbon-rich stars under a wide variety of temperature and pressure.[23] Therefore, PAHs have significant importance astrochemically. Benzene is the simplest building block of polycyclic aromatic hydrocarbons (PAHs) and soot platelets. But formation mechanism of benzene in the interstellar medium is elusive for decades now. Recently, in 2004, propenal, which is also popularly referred to as acrolein, has been detected in the interstellar medium. Thus, there is a high probability of finding propargyl alcohol in ISM too, which is a more stable structural isomer of propenal. Propargyl alcohol has gained astrochemical importance since two propargyl radicals can form benzene (Figure 2) which can be one of the possible ways proposed of benzene formation in ISM. Thus, the study of propargyl alcohol is of great interest to astrochemists.

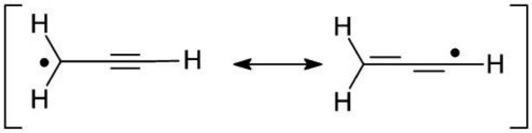

Figure 2a: Propargyl radical

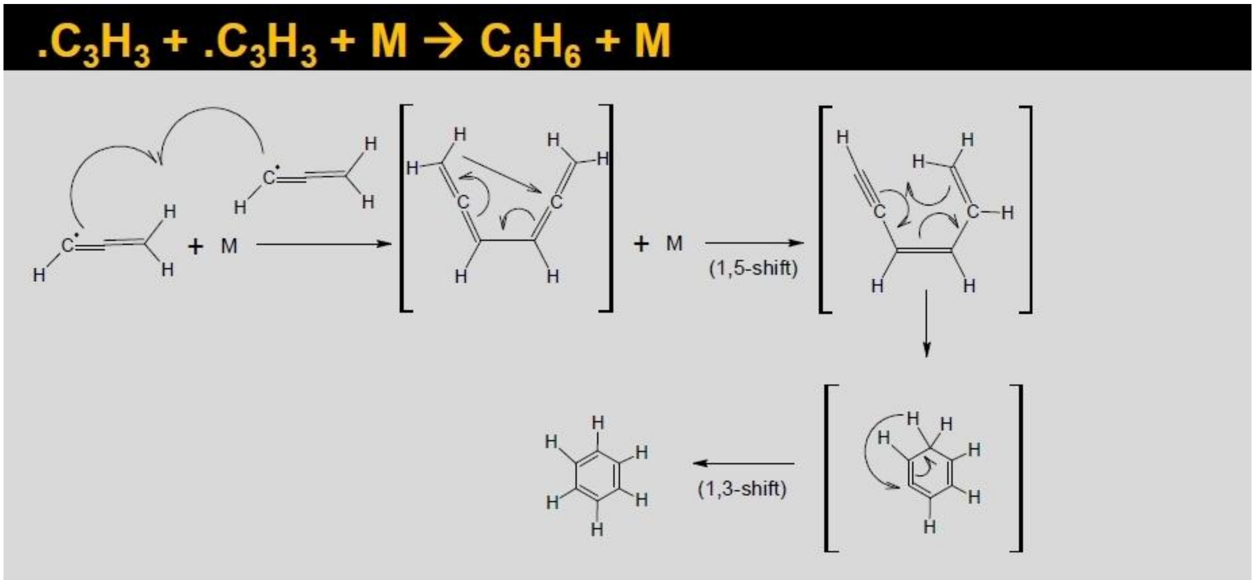

Figure 2b: Formation of benzene through propargyl radical pathway [26]

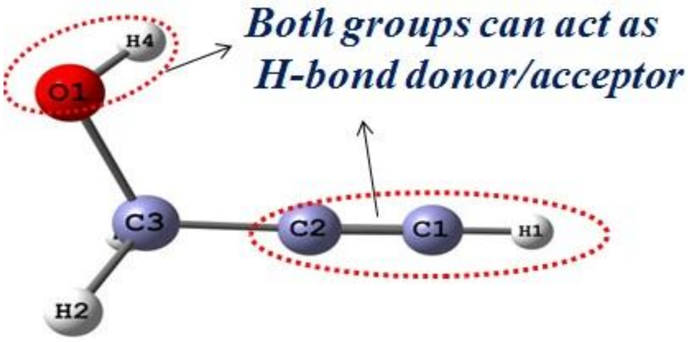

Figure 3: Hydrogen bonding sites in propargyl alcohol

Furthermore, propargyl alcohol has an O-H group and a C≡C-H group. Thus it has multiple hydrogen bonding sites and competitive H-bonding can be studied (Figure 3). Its interaction with some other molecule with strong dipole moment can be studied were we get various complexes for the different interacting sites. The groups can act as proton donor or acceptor depending on the nature of the other molecule that it is interacting with. Thus, it is possible to have multiple minima on the potential energy curve.

Methyl amine is also a good candidate as an interstellar molecule and was first identified in 1974 in interstellar clouds. [24] MA has an electronegative nitrogen that can accept the O-H hydrogen or the C≡C-H acidic hydrogen, in propargyl alcohol. Also, though a weak donor, there is a possibility of hydrogen donation from the amine group to oxygen or the π-cloud of propargyl alcohol. Nitrogen as a proton donor in hydrogen bonding is seen in various biological system (Figure 1a). Molecules with multifunctional sites therefore afford the possibility of a number of complexes and the preferences for the formation of each of the structures poses an interesting and complex study. Studying these complexes gives an idea of which interaction is most stable and what complexes may be present in the ices in the interstellar medium.

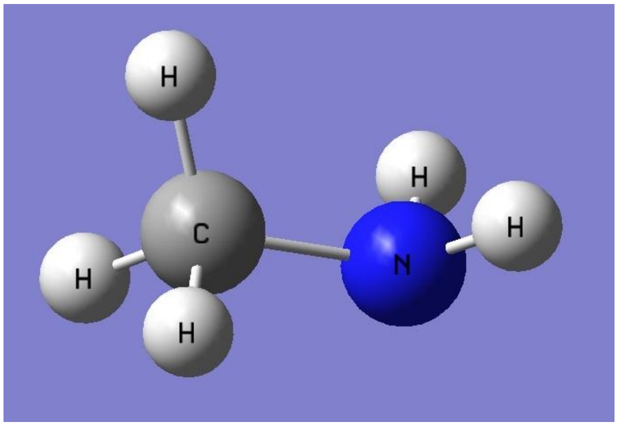

Fig. 4: Methyl amine

1.4 Status of Current Research

Various spectroscopic studies have been carried out on propargyl alcohol; which focus on the vibration-rotation interaction and intra-molecular vibrational energy redistribution in the ground state. Structures and dynamics of propargyl alcohol, in its ground electronic state, have also been studied widely.[3.] Also, theoretical studies have been carried out which computes the reaction of propargyl radical to form benzene through radical addition.[4.]Methyl amine studies have been carried out in matrix isolation by Purnell et. al.[21.]Also, interaction energies and structural parameters of methyl amine complexes with water have been studied computationally by Mmereki and Donaldson. [25.]

Scope and Objectives of the Present Work

This thesis provides a report on the study of the possible interactions between propargyl alcohol and methyl amine; and between methyl amine and water. Different computational methods such as Gaussian 09 and AIM analysis were used to find out possible complexes of the two paired molecules. To study these complexes experimentally, matrix isolation infrared spectroscopy is used. It provides an excellent method to study systems with H-bonds as it can trap local minima in addition to the global minimum. Another advantage is the narrow bandwidth that this technique provides which can resolve the bands which otherwise are overlapped in the condensed phase.

Chapter 2: Experimental and Computational Procedures

The matrix isolation experimental set up and the computational methodology employed to study the hydrogen bonded complexes of propargyl alcohol with methyl amine and methyl amine with water are described in this chapter.

2.1 Matrix Isolation Technique

Matrix isolation is an experimental technique in which a substrate is mixed with a large excess of an inert gas and is condensed on a surface that is sufficiently cold (~12K) to assure rapid solidification of the mixture.[5.] The large excess of the inert gas ensures that the molecule of interest is trapped isolated in the solid host. Each substrate molecule is immobilized in a cavity surrounded by one or more layers of the inert material and thus is 'isolated' from the other substrate molecules in a 'matrix' of the host gas and we get a sample for study. To be sure of attaining isolation, typical matrix to substrate ratios used are between 10^3:1 and 10^5:1. This avoids aggregation of the isolated molecule. The term 'matrix isolation' was coined by George Pimentel who initiated this field for the characterization of reactive intermediates and other unstable or transient species by spectroscopy, which by virtue of they being trapped isolated in an inert cage have almost infinite lifetimes for want of a reaction partner.[6.]Though the technique was developed by Pimentel and his co-workers for the study of reactive species, it is a powerful tool for the study of weakly bound complexes and conformations of molecules as well.

The host gases used in the matrix isolation technique are generally inert gases or nitrogen, that do not react with the substrate. In addition to their chemical inertness, these gases satisfy certain properties such as optical transparency in the region of interest, low volatility at the temperature of study, low latent heat of fusion and acceptable thermal conductivity. Once the matrix isolated sample is prepared (Figure 5), it is deposited onto a cold KBr or CsI window if the sample is to be studied using infrared spectroscopy. Quartz is the material of choice for the window material if UV-visible or fluorescence is the technique to be used for probing the trapped molecules. There have also been many studies using electron spin resonance spectroscopy where the deposition is usually done on sapphire-tipped copper rods.

The molecule under study must have a vapor pressure of a few millitorr at easily attainable temperatures (77 K to ~300 K) so that it can be mixed with the inert gas by standard manometric techniques. It is an experimental challenge to deposit molecules with extremely low pressures, at easily attainable temperatures, since heating such samples to high temperatures to generate reasonable vapor pressures may sometimes lead to their decomposition. Laser ablation has been used for such studies, but with limited scope.

The temperature of deposition of the matrix should be below 30% of the melting point of the gas being used (30 K for Argon; 35 K for N_2). Typically, 10 K is used which is well below the limit required.

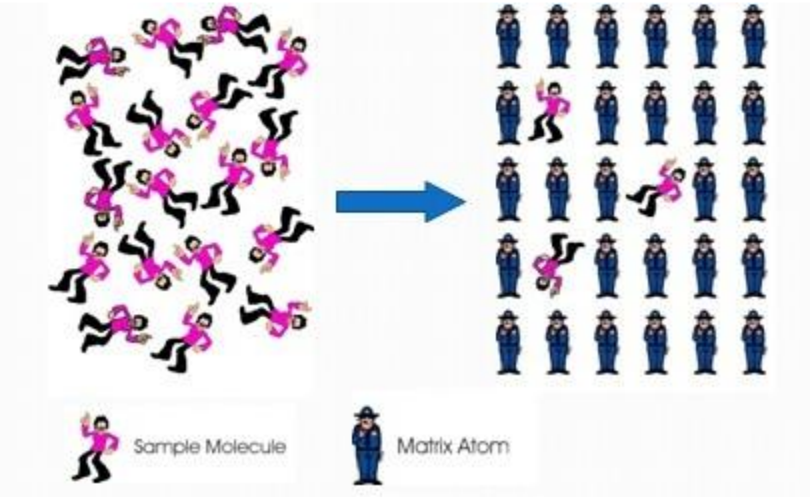

Figure 5: A schematic showing trapping of molecules in a matrix

2.2 Advantages

In the matrix isolation technique, since the substrate is surrounded with an inert matrix, they do not experience any significant intermolecular interactions. In addition, since the substrate is isolated from each other and are immobilized, there will be no collisional and Doppler broadening. Furthermore, trapping of the molecules at very low temperatures ensures that only the lowest electronic and vibrational levels are populated. As a result of all the factors mentioned above, the spectra of the matrix isolated samples generally show linewidths that are significantly smaller than those obtained for condensed or vapor phase samples.

Where short-lived systems, such as radicals, are trapped in the matrix, this technique yields detailed insight into the electronic and, often indirectly, the molecular structure of the reactive intermediates.

2.3 Matrix Environment Effects

Though the matrix is considered to be inert, it is not uncommon to observe the spectra of the trapped species being perturbed by the matrix. These matrix effects are evident through changes in vibrational frequencies, shapes and intensities. In some cases it causes a single vibrational mode to show multiplet structure. We discuss below some of the effects.

1. Matrix shifts -

The substrate molecules, trapped in the matrix, experience weak interactions with the matrix which result in either a shift in the frequency or splitting of the bands. The frequency shift, with respect to the gas phase value, arises from electrostatic, inductive, dispersive and repulsive interactions. Argon, nitrogen gases cause only small shifts (<1%) in the infrared features of the molecules as compared to their gas phase values. It has been observed that a tight cage usually shows a blue shift; and a loose cage a red shift.

2. Multiple trapping sites-

In the matrix, the substrate is trapped either in the interstitial holes or in the substitutional sites. Depending on the site the substrate is trapped in, it will experience intermolecular forces to varying degrees. Therefore, different matrix cages might induce different shifts in the band. Also, the intensity due to substrates trapped in different sites varies according to the stability of the trapping site. This effect can be discerned by changing the matrix, since it is very unlikely that two different matrices would give rise to same trapping sites.

3. Aggregation-

The experiments of matrix isolation are carried out generally with the matrix to substrate ratio of 1000:1. Higher concentrations of the substrate may result in formation of molecular aggregates such as dimers, trimers and higher multimers along with the monomers. The features arising due to this aggregation or self- association are generally identified by performing a concentration dependence experiments.

4. Molecular rotation-

Usually in the frozen matrix free rotations are inhibited. But rotations have been observed in case of small molecules such as water and ammonia. These can be identified through temperature cycling experiments wherein the features corresponding to rotations will show reversible intensity changes.

2.4 Instrumentation Aspects

The matrix isolation infrared spectroscopy set up consists of a cryostat, a vacuum system and an FTIR spectrometer as its main components, as shown in Figure 6. Each component is explained below in brief.

2.4.1 Cryostat

A cryostat is used to produce cryogenic temperature which is required to solidify the inert gas and helps it to form a matrix. These low temperatures are also important to avoid diffusion of trapped species. Low temperatures of 77 K, 20 K and 10 K are achieved using micro refrigerators with nitrogen, hydrogen and helium as working fluids respectively. The micro refrigerators can also attain higher temperatures just by changing the rate of heat extraction. This phenomenon is very useful to carry out controlled annealing and diffusion in the matrix.

Our system is equipped with a closed cycle helium compressor (Figure 7) cooled cryostat **CH-202w/HC4E1** Model (Sumitomo Heavy Industries Ltd.) which can attain a low temperature of 10K (Figure 8). The Helium compressor was cooled by a 3 kW chiller unit which supplied cold water to remove the excess heat generated in the compressor.

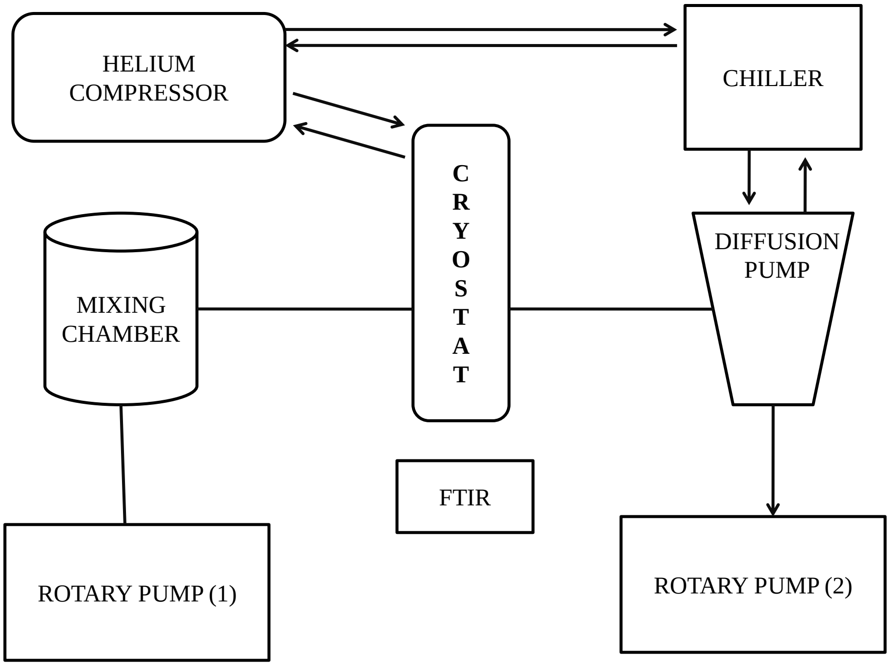

Figure 6: A schematic of the matrix isolation Infrared spectroscopy set up

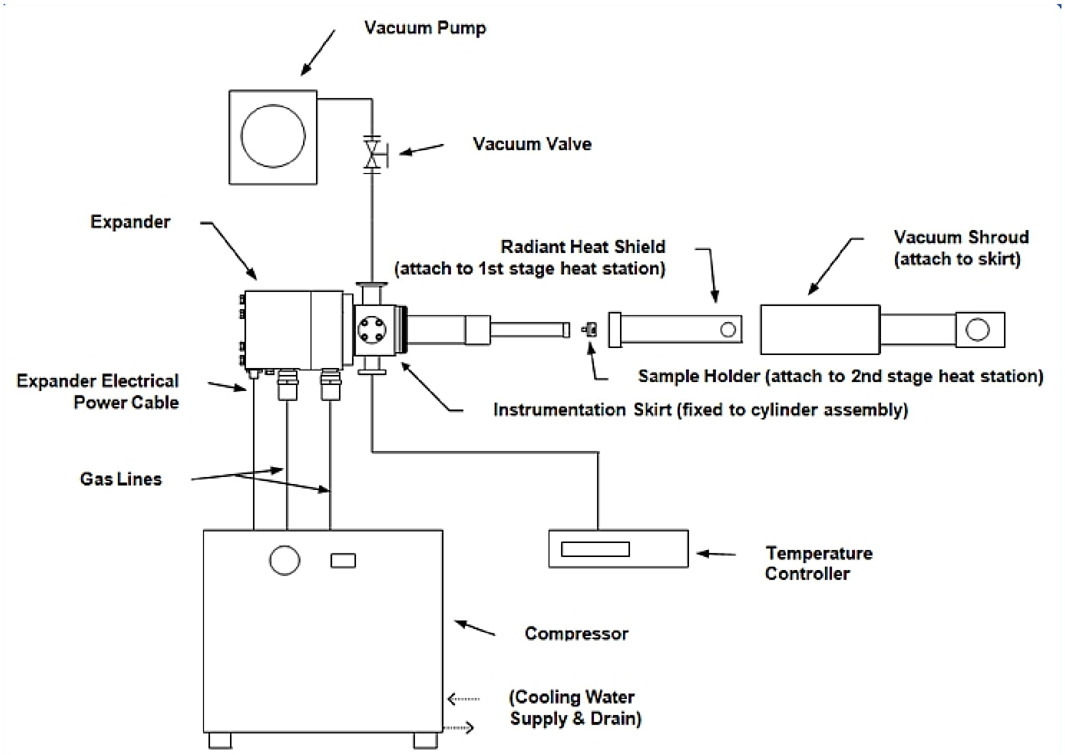

Figure 7: Set up of a closed-cycle helium cryocooler[7.]

Figure 8: Photograph of helium compressor cooled cryostat in our experimental set up [23.]

2.4.2 Vacuum system

In our vacuum system, Edwards Diffstak MK2 series diffusion pump (Figure 9) is incorporated which has a pumping speed of around 280 L/s for air. This pump was backed with a rotary pump of capacity 300 L/min. The base vacuum obtained is 10^{-6} mbar at room temperature and 10^{-7} at 12 K and is measured using a cold cathode gauge (MKS vacuum Product I-Mag). For the effective working of the diffusion pump, it was cooled with chilled water at 15 ^{o}C, obtained using a 3 kW chiller. The various accessories which were used in order to create an effective system are shown in the figure 10.

Figure 9: Photograph of the diffusion pump in our vacuum system

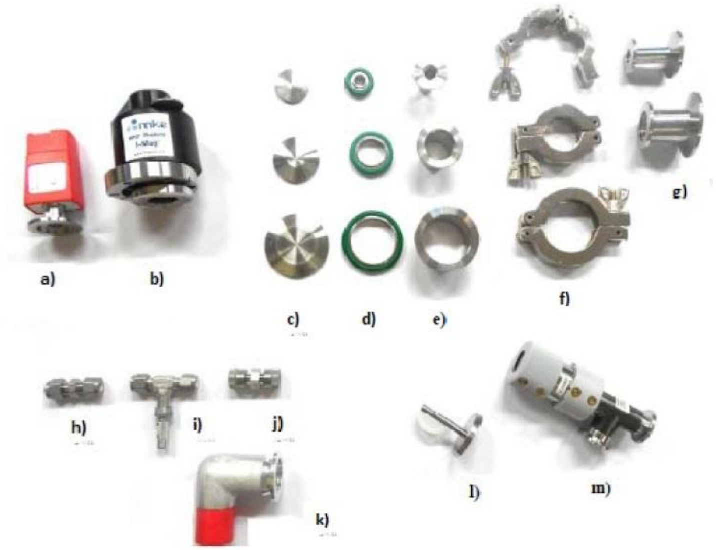

Figure 10: Photographs of the various vacuum components used in our setup[23]. a) Pirani gauge b) Cold cathode gauge c) Dummy KF 40/25/10 d) O Rings KF40/25/10 e) KF 40/25/10 Flanges f) KF 40/25/10 Clamps g) KF 25-10,KF 40-25 Reducers h) Swagelok Straight fitting i) Swagelok metering valve (T shaped) j) Swagelok connectors k) KF 25 Right Angle Flange l) Single jet (effusive nozzle) m) High precision needle valve

2.4.5 Pressure Measurements:

The pressure in the vacuum system varies over many orders of magnitude at various experimental stages. Therefore, it is measured using different types of gauges appropriate for the different pressure regimes. The gauges used in our vacuum system are described below.

2.4.5.1 Capacitance Manometers - A capacitance manometer is a diaphragm manometer where the gauge head is divided into two chambers by a thin metal diaphragm that serves as one plate of a capacitor. The second plate of the capacitor is fixed in one of the chambers. A change in the pressure difference between the two chambers results in a change in capacitance as the flexible diaphragm moves relative to the fixed plate. A sensitive capacitance bridge measures the capacitance between the two plates and the capacitance is converted to a reading of the pressure difference. A capacitance manometer is designed so that the flexible diaphragm touches the opposing capacitor plate at a small overpressure. This protects the fragile diaphragm from a sudden thrust of gas. As might be expected, the capacitance measurement is very sensitive to the temperature of the flexible diaphragm. High precision gauge heads incorporate a heater and temperature control that maintains the gauge head at a constant temperature. Capacitance manometers are available to measure pressures from 1000 torr down to less than 10^{-4} torr.[9.]

2.4.5.2 Thermal-Conductivity Gauges - The thermal conductivity of a gas decreases above some constant value, about 10 torr and reaches essentially zero at about 10^{-3} torr.[9.]This change in thermal conductivity is used as an indication of pressure in the Pirani gauge and the thermocouple gauge. In both gauges a wire filament is heated by the passage of an electrical current. The temperature of the filament depends on the rate of heat loss to the surrounding gas. In the Pirani gauge, the heated filament is one arm of a Wheatstone bridge. A change in temperature of the filament produces a change of resistivity and hence a change in the voltage across the filament. The resulting imbalance of the bridge gives an indication of pressure. Usually, a voltage is applied to keep the bridge in balance and this voltage serves as an indicator of the pressure. The pressure indicated by a Pirani gauge depends upon the thermal conductivity of the gas. They are usually calibrated by the manufacturer for use with air. For other gases these gauges must be recalibrated over their entire range, since thermal conductivity is a nonlinear function of pressure. This accuracy is adequate when the gauge is used to sense the fore-line pressure of a diffusion pump or to determine whether the pressure in a system is sufficiently low to turn on a diffusion pump. The principal advantages of these gauges are ease of use, ruggedness and low cost.

2.4.5.3 Ionization Gauges - In the cold cathode gauge an electrical discharge is struck in a low-pressure gas between two electrodes maintained at a potential difference of several kV. In order to provide stability as well as to confine the path of the electron in the discharge, a magnetic field is applied in the gauge head. The discharge current measured at one of the electrodes provides a measure of the gas pressure. Cold cathode gauges operate in the 10^{-2} to 10^{-7} torr range with an accuracy of a factor of two at best.[9.] Cold cathode gauges are robust and economical, suffering primarily only from their limited range of applicability. Cold cathode gauge in various configurations are referred to as Penning gauges, magnetrons and inverted magnetrons.

2.5 Fourier Transformation Infrared Spectrometer (FTIR)

The vibrational spectra of molecules trapped in the matrix were recorded using a Bruker Tensor 27 FTIR spectrometer (Figure 11). This spectrometer is usually operated at a resolution of 0.5 cm^{-1} and typically 8 scans are co-added to obtain a good signal-to-noise ratio. All the spectra are recorded in the region of 4000 to 400 cm^{-1}. At the time of annealing (explained in procedure part), heater-temperature controller unit (Lakeshore Instruments) was used to maintain the matrix at required temperatures.

2.6 ANALYTE INTRODUCTION

The basic requirement for conducting a MI experiment of a desired sample is that the compound should possess a vapor pressure large enough for deposition. Compounds which have a low vapor pressure are heated whereas compounds with high vapor pressures are cooled to obtain the desired vapor pressure for deposition. To start with, a mixture of analyte and matrix was prepared in a stainless steel mixing chamber of one liter capacity, which was introduced to the vacuum system through a single effusive nozzle, also known as single jet nozzle. There are also other sources by which desired samples are introduced in the vacuum system; viz., double jet effusive nozzle and hot nozzle source. A hot nozzle source is usually used to identify the vibrational features for higher energy structures.

2.7 EXPERIMENTAL PROCEDURE

Before the experiment is started; it was made sure that the vacuum in the system was in the realm of 1 x 10^{-6} torr. The sample holder was thoroughly degassed and then the sample was loaded into the holder. The sample was then subjected to several freeze-pump-thaw cycles to ensure that the sample was thoroughly degassed. To obtain the desired matrix to sample ratios, the required vapor

Figure 11: Photograph of the matrix isolation set up – A) Cryostat B) Diffusion Pump C) Mixing Chamber D) Rotary Pump E) Nitrogen gas cylinder F) FTIR spectrometer G) Temperature controller

pressure of the sample was calculated, which was then obtained by maintaining the sample at the appropriate temperatures. The appropriate temperatures were calculated using the Clausius- Clapyron Equation (Eq. 1),

$$\boldsymbol{ln\frac{P_2}{P_1} = \frac{\Delta H}{R}(\frac{1}{T_1} - \frac{1}{T_2})} \quad (1)$$

where P_1 *and* P_2 are vapor pressures at temperatures T_1 *and* T_2 respectively, R is gas constant with value of 8.314 J/K/mol and ΔH the heat of vaporization .

The samples were equilibrated at required temperature, for about an hour, to obtain the desired vapor pressure of the sample and streamed into a stainless steel mixing chamber. The temperature of the cold bath was measured using a platinum resistance thermometer. The mixing chamber of one litre capacity was used to prepare the matrix/sample gas mixtures. When performing an experiment for the interaction between two sample molecules, the sample molecules where filled sequentially into the mixing chamber. The chamber was then filled with matrix gas and allowed to equilibrate for about ten minutes. The sample with the matrix gas was then allowed to deposit on the cold KBr substrate maintained at 12 K. The rate of deposition was controlled using a fine needle valve which was set at a value of 230.

After the matrix was deposited, a spectrum was recorded. The temperature of the matrix was then raised to either 30 K or 35 K depending on whether N_2 or Ar is used as matrix gas. The matrix was kept at this temperature for about half an hour using the heater-temperature controller unit followed by recording a spectrum. It was then cooled back to 12 K and a spectrum was recorded. This process of heating the matrix followed by cooling is called annealing. The matrix was usually annealed for about 2 hrs. Annealing helps in removing unstable sites in the matrix and also encourages diffusion of the precursor molecules to form adducts.

2.8 QUANTUM CHEMICAL COMPUTATIONS

2.8.1 Geometry optimization and frequency calculations

At the outset, the structure of a molecule or complex corresponding to a minimum on the potential surface is achieved by geometry optimization. A geometry optimization protocol starts by making an initial guess of the molecular structure which is given as input. The energy and gradient are calculated at the point on the potential surface corresponding to the initial geometry and then this information is used to determine in which direction and to what extent the next step should be taken to improve the geometry. At the minimum in the potential energy curve all the forces will be zero. In the case of Gaussian software package the minimum energy structure of the molecules is achieved when the forces, the root mean square of forces, the calculated displacement and the root mean square of the displacement for the subsequent step are below specified threshold values.

Geometry optimization calculations were performed at various levels of theories, namely Hartree-Fock (HF) , Møller-Plesset second order perturbation (MP2) and Density Functional Theory (DFT- B3LYP, M06-2x) and using various basis sets[STO-3G, 6-31G, 6-311G++(d,p)]. The B3LYP method uses the Becke three parameter non-local exchange functional[10,11] with non-local correlation of Lee et al. [12.] Vibrational frequency calculations were performed at the same level of theory which was used for optimization. The vibration computations were performed in order to confirm that the structures obtained indeed correspond to minimum in the potential surface and also to assign the vibrational features observed in the experiments. The computed vibrational frequencies were scaled to bring them in agreement with experimental results. In order to determine the scaling factor the experimentally observed strongest feature was correlated with the computed strongest feature. The scaling factor which would bring the computed frequency in good agreement with that of experiment was used to scale all other vibrational frequencies. Zero point vibrational energies (ZPE) were also obtained from the frequency calculation and which was used to calculate the ZPE corrected energies for the various complexes.

2.8.2 Stabilization energy calculation of complexes

The stabilization energy or the interaction energy E of a complex is given by the equation 2

$$\mathbf{E = E_{AB} - (E_A + E_B)} \qquad (2)$$

where E_A, E_B and E_{AB} represent energies of monomer A, monomer B and complex AB respectively. Negative value of E signifies that the complex is more stable relative to the precursors. The stabilization energy of the complex corrected for zero point energy (ZPE) was also calculated. ZPE is the energy that a molecule possesses even at absolute zero temperature. Stabilization energies to be experimentally meaningful must be corrected for the ZPE, as follows-

$$\mathbf{E_{total} = E_{cal} + ZPE} \qquad (3)$$

where E_{total} is the stabilization energy after ZPE correction i.e. at v=0 level and E_{cal} is the stabilization energy at the bottom of the potential curve.

When the energy of complex (E_{AB}) is computed, the basis functions used are those of both the monomer subunits. However, for computing the energy of the individual precursors (i.e. E_A and E_B), the basis functions are those of the precursors used. Since the number of basis functions is larger in the computation of the complex than for the individual precursors, the energy obtained will be lowered, due to the fact that each monomer can now use the basic functions of other. Stabilization energies thus derived from the calculated energies E_A, E_B and E_{AB} will be overestimated and the error is referred to as the basis set superposition error (BSSE).[13-17] The best way to eliminate the BSSE is to increase the basis set until the stabilization energy is the desired minimum with the tradeoffs of large computation times for even small systems. The commonly used method to correct for BSSE is through the use of the counterpoise correction method proposed by Boys and Bernadi. In this scheme, all the energies of monomer E_A, E_B and the complex E_{AB} are computed in the same basis set spanned by the functions of the complex AB. The stabilization energies are then obtained as follows

$$\mathbf{E = E_{AB}\,(AB) - \{E_A\,(AB) + E_B(AB)\}} \qquad (4)$$

where, E_A (AB) = Energy of the monomer A using the basis set AB, E_B (AB) = Energy of the monomer B using the basis set AB and E_{AB} (AB) = Energy of the complex AB using the basis set AB

In our studies, the stabilization energies of the complex corrected for the BSSE have also been included. Corrections of energies for ZPE and BSSE simultaneously were not included as these values are known to overcorrect the stabilization values.[18, 19]

2.8.3 Atoms-in-molecules (AIM) methodology –

The atoms in molecules theory was first proposed by Bader which is based on electron density topology. For performing the (AIM) analysis the wave functions corresponding to the optimized geometry of a molecule or complex are generated using the Gaussian package.[20.] From the electron density plot one can obtain the bond critical points, charge density ρ, Laplacian of charge density $\nabla^2\rho$, which is also the trace of the Hessian of ρ. The charge density, ρ(r), is a physical quantity which has a definite value at each point in space. Each topological feature of ρ(r), where it is a maximum, a minimum, or a saddle point, is associated with a space called a critical point, where the first derivative of ρ(r) vanishes. The sign of the second derivative at this point determine whether the function is maximum or minimum. The topological properties of such a scalar field are conveniently summarized in terms of the number and nature of its critical points. The rank of critical point, denoted by ω, is equal to the number of non-zero eigen values or non-zero curvature of ρ at the critical point. The signature denoted by σ, is the algebraic sum of the signs of the eigen values. The critical point (CP) is labeled by giving the values (ω, σ). For example, (3, -1) critical point means, three non-zero curvatures and one positive and two negative eigen values. A (3, -1) CP corresponds to a bond between two atoms, a (3, +1) CP to a ring, a (3, +3) CP to a cage and a (3, -3) CP corresponds to a maximum. The numbers of critical points of all types, which can co-exist in a system with a finite number of nuclei, are governed by the Poincare-Hopf relationship:

$$\mathbf{n - b + r - c = 1} \tag{5}$$

where n is the number of nuclei, b is the number of bond critical points, r is the number of ring critical points and c is the number of cage critical points.

The sum of three Hessians (λ1, λ2, λ3) at a bond critical point, the quantity $\nabla^2\rho$ provides a useful characterization of the manner in which the electronic charge density is distributed in the inter nuclear region. If the value of charge density ρ ($<10^{-1}$ au) and the curvature of charge density are large, Laplacian of charge density may be positive or negative usually in the same order of magnitude as ρ then the interaction is of shared type, typical of covalent interaction. For the closed shell interactions, such as hydrogen bond complexes, van der Waals complexes and ionic systems, the charge density ρ ($\sim10^{-2}$ to 10^{-3} au) at the bond critical point is quite small and the Laplacian of the charge density is positive.

Chapter 3: Study of propargyl alcohol complexes with methyl amine

3.1 EXPERIMENTS

Propargyl alcohol and methyl amine hydrogen bonded complexes were studied using matrix isolation infrared spectroscopy in nitrogen matrix at 12 K. The details of the experiments are described below. Experiments were carried out in nitrogen as well as argon matrices. The results obtained in Ar matrix are not presented below since the results in Ar matrix were not very different than the results in N_2 matrix.

3.1.1 Matrix isolation infrared spectrum of propargyl alcohol

IR spectra of propargyl alcohol were recorded in nitrogen matrix at various concentrations ranging from 1mbar - 10 mbar mixed with 1000 mbar of matrix gas. The major features seen in the propargyl alcohol spectra, which increase on increase in PA concentration, are shown in figure 12.

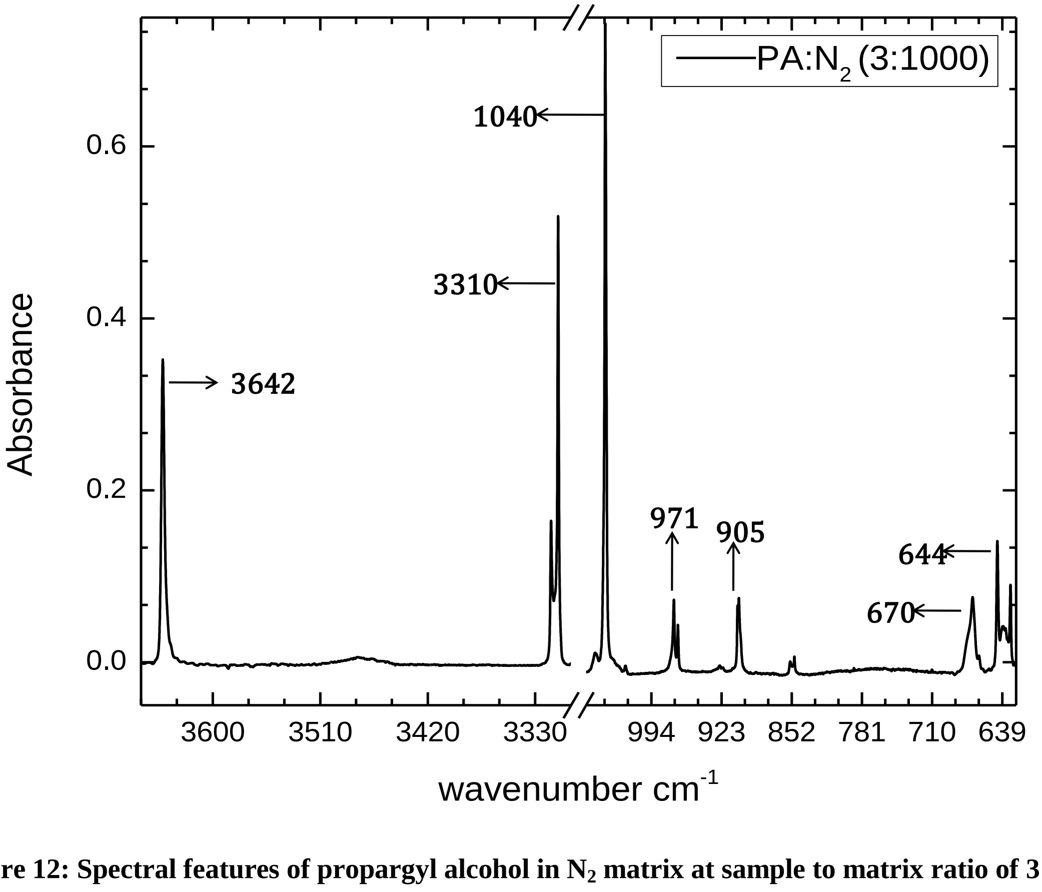

Figure 12: Spectral features of propargyl alcohol in N_2 matrix at sample to matrix ratio of 3:1000

3.1.2 Matrix isolation infrared spectrum of methyl amine

Methyl amine has very high vapor pressure at room temperature. In order to obtain vapor pressures of 0.8, 1.3, 1.9 and 3 mbar, methyl amine was maintained at -70, -60, -50 and -36 ^{o}C temperatures respectively. In the experiments, the sample to matrix ratio was 0.8:1000, 1.3:1000, 1.9:1000 or 3:1000. The major spectral features of methyl amine are shown in figure 13.

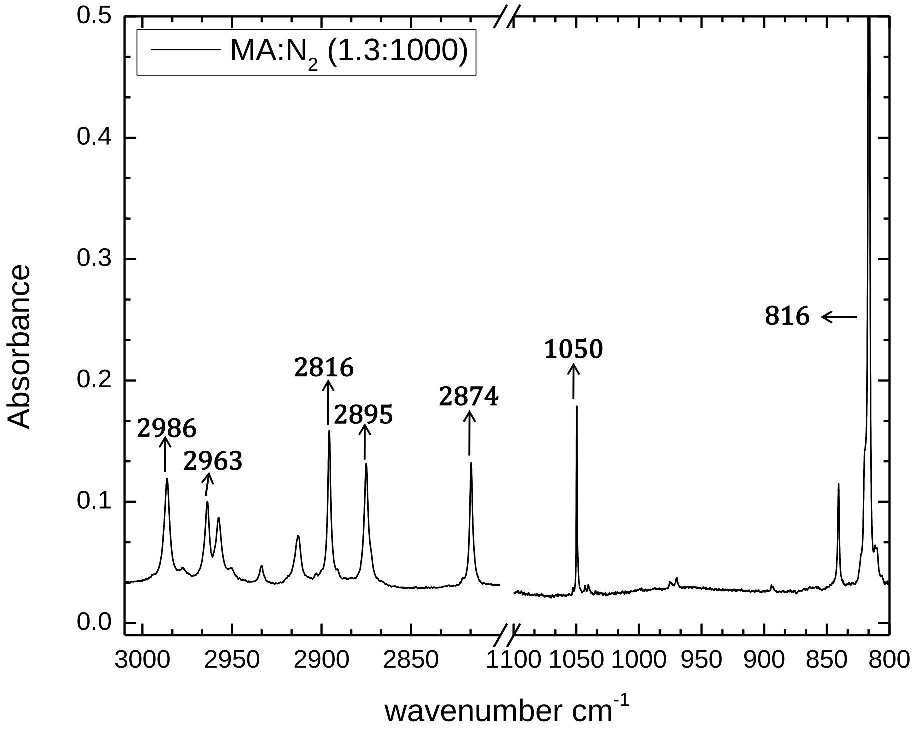

Figure 13: Spectral features of methyl amine in N_2 matrix at sample to matrix ratio of 1.3:1000

3.1.3 Matrix isolation infrared spectrum study of propargyl alcohol and methyl amine

Propargyl alcohol and methyl amine in various ratios were together mixed in ~1000 mbar of nitrogen. New features exclusively seen *only* in the presence of both the molecules, and which therefore correspond to product bands, are shown in figure 14. The product features have been labeled C3 and C4; the identity of C3 and C4 will be explained later.

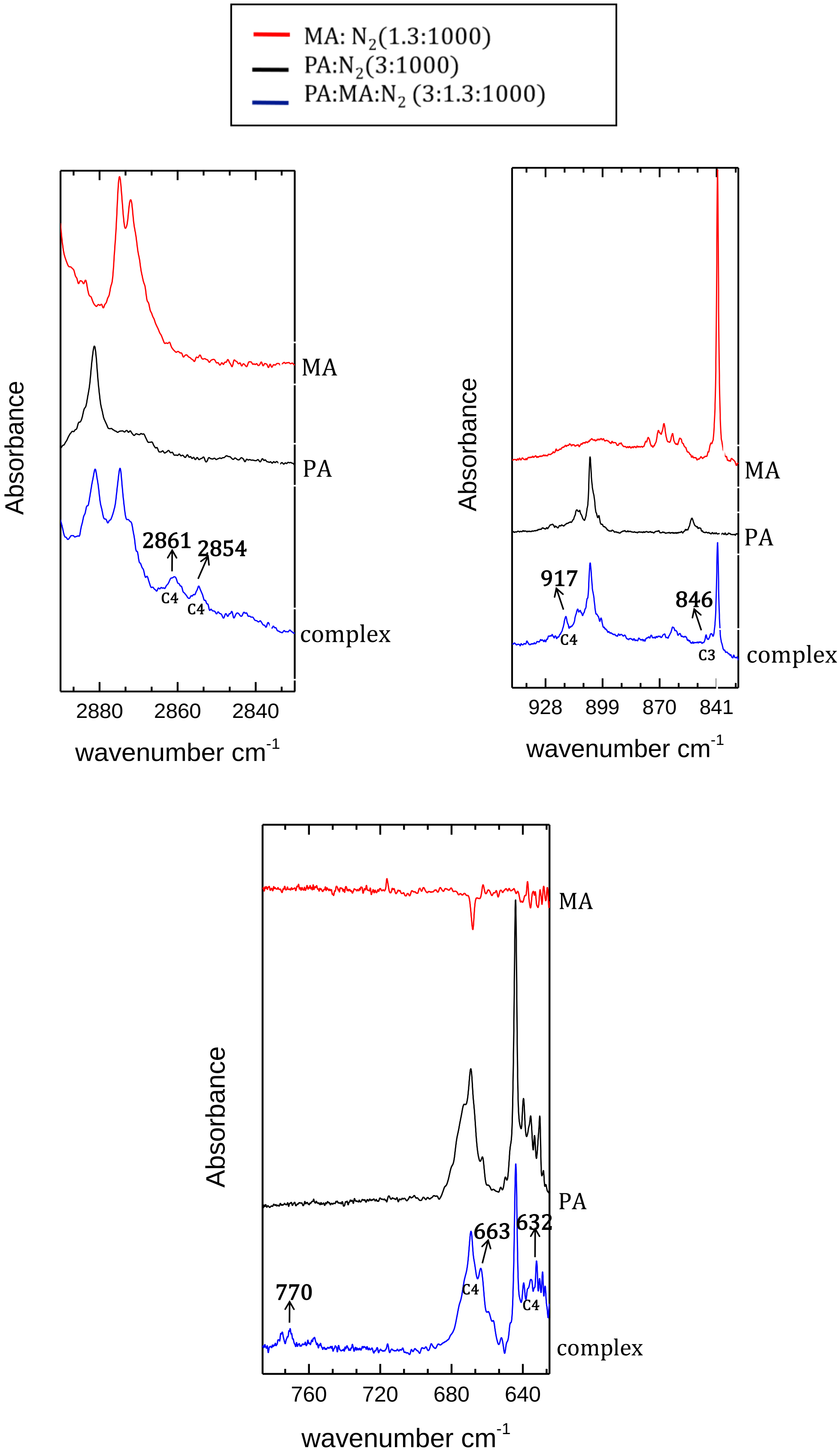

Figure 14: New spectral features seen in propargyl alcohol with methyl amine in N_2 matrix experiments after 30 min of annealing with PA:MA:N_2 (3:1.3:1000)

3.2 COMPUTATIONS

Complexes of propargyl alcohol with methyl amine were also studied using computational techniques. The possible structures are listed below:

1. Complex 1 – Hydrogen bonded complex with nitrogen in methyl amine acting as a H-bond donor to the acetylene π cloud in propargyl alcohol
2. Complex 2 – Hydrogen bonded complex with nitrogen in methyl amine acting as a H-bond donor to oxygen in propargyl alcohol
3. Complex 3 – Hydrogen bonded complex with acetylene group in propargyl alcohol acting as a H-bond donor to nitrogen in methyl amine
4. Complex 4 – Hydrogen bonded complex with oxygen in propargyl alcohol acting as a H-bond donor to nitrogen in methyl amine

The above structures are intuitive and it is necessary to find out if the above structures are indeed minima on the potential surface and which one represents the global minimum. The optimization and frequency calculations were done at various levels of theory viz., B3LYP, M06, MP2; using the 6-311++G(d,p) basis set.

All complexes obtained at B3LYP/6-311++G(d,p) level of theory are shown in figure 15. The bond parameters obtained for these complexes are indicated in Table 1. Their stabilization energies along with ZPE (zero point energy) and BSSE corrections are tabulated in Table 2. At this level of theory complex 4 is the most stable one for propargyl alcohol – methyl amine followed by complex 3, 2 and 1. ZPE and BSSE corrections are not applied together to determine the interaction energies because application of the combined correction has been shown to overcorrect.[18.]

The same basis set was used to calculate frequencies for these complexes. For all complexes, frequencies were found to be positive, which confirms that the structures obtained are indeed minima on the potential energy surface. The frequency calculations at B3LYP level have been used through out to identify peaks, find out scaling factors for the prominent vibrations in monomers and then corresponding vibrations in the complexes. In the complexes obtained at this level, the O-H stretching modes were red shifted. The C-O stretching mode for complex 4, i.e. the most stable one was blue shifted, while this mode for the other three complexes of propargyl alcohol-methyl amine were red shifted. The computed spectra for the four complexes of propargyl alcohol – methyl amine are shown in figure 16.

Table 1: Important structural complex parameters – bond lengths (Å), bond angles (^{o}) and torsional angles (^{o}) of various complexes shown in Fig. 15; of propargyl alcohol and methyl amine computed at B3LYP/6-311++G(d,p)

Complex parameters	Complex 1	Complex 2	Complex 3	Complex 4
O3 – H8	0.96	0.96	0.96	0.98
O3 – C1	1.42	1.43	1.43	1.41
C6 – H7	1.06	1.06	1.07	1.06
C5 – C6	1.20	1.20	1.20	1.20
N9 – C12	1.46	1.46	1.47	1.47
N9 – H10	1.01	1.01	1.01	1.01
N9 – H8	2.55			1.87
N9 – H7			2.24	
N9 – H4		2.60		
O3 – H10		2.26		
C5 – H11	2.92			
C1 – O3 – H8	108.3	108.8	108.1	108.4
C12 – N9- H10	113.5	111.1	110.6	110.8
H2 – C1 – O3 – H8	72.1	72.4	75.4	-55.8
O3 – H8 – N9 – C12	-141.5			73.6
H11 – N9 – C12 – H15	-63.5	59.2	62.5	67.1
O3 – C1 – N9 – C12	93.3	94.2	16.0	

Table 2: Stabilization Energies at B3LYP using 6-311++G(d, p)

Complex	#	ΔE_{Raw} , ΔE_{ZPE} , ΔE_{BSSE} (kcal/mol)
PA-MA (H ⋮ C≡C)	1	-8.3, -6.7, -7.6
PA-MA (N-H···O)	2	-3.8, -2.7, -3.4
PA-MA C≡C-H…N)	3	-3.0, -2.0, -2.7
PA-MA (O-H…N)	4	-0.7, -0.2, -0.5

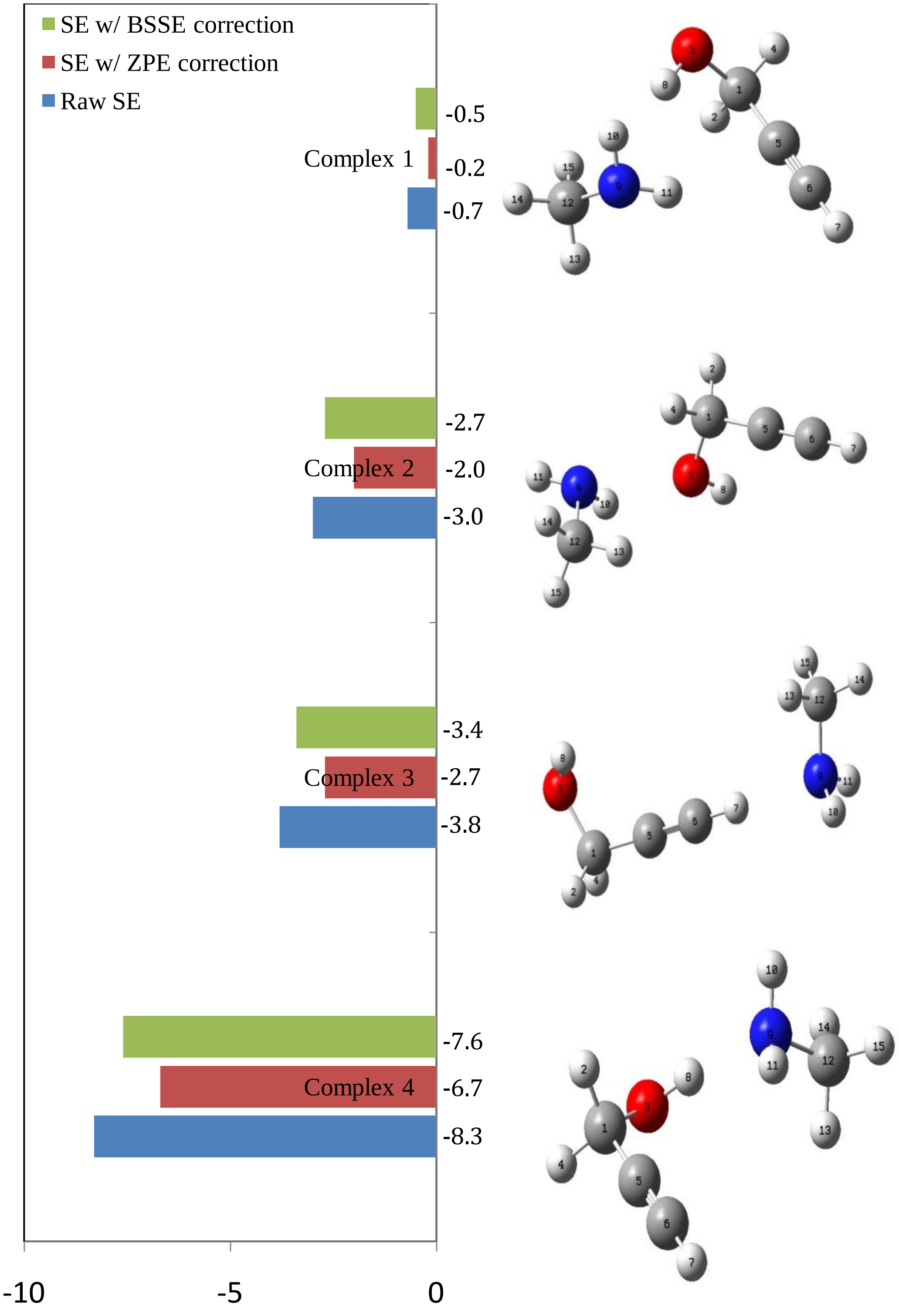

Figure 15: Optimized geometry structures obtained at B3LYP using 6-311++G(d, p) with their stabilization energies for complexes of propargyl alcohol with methyl amine

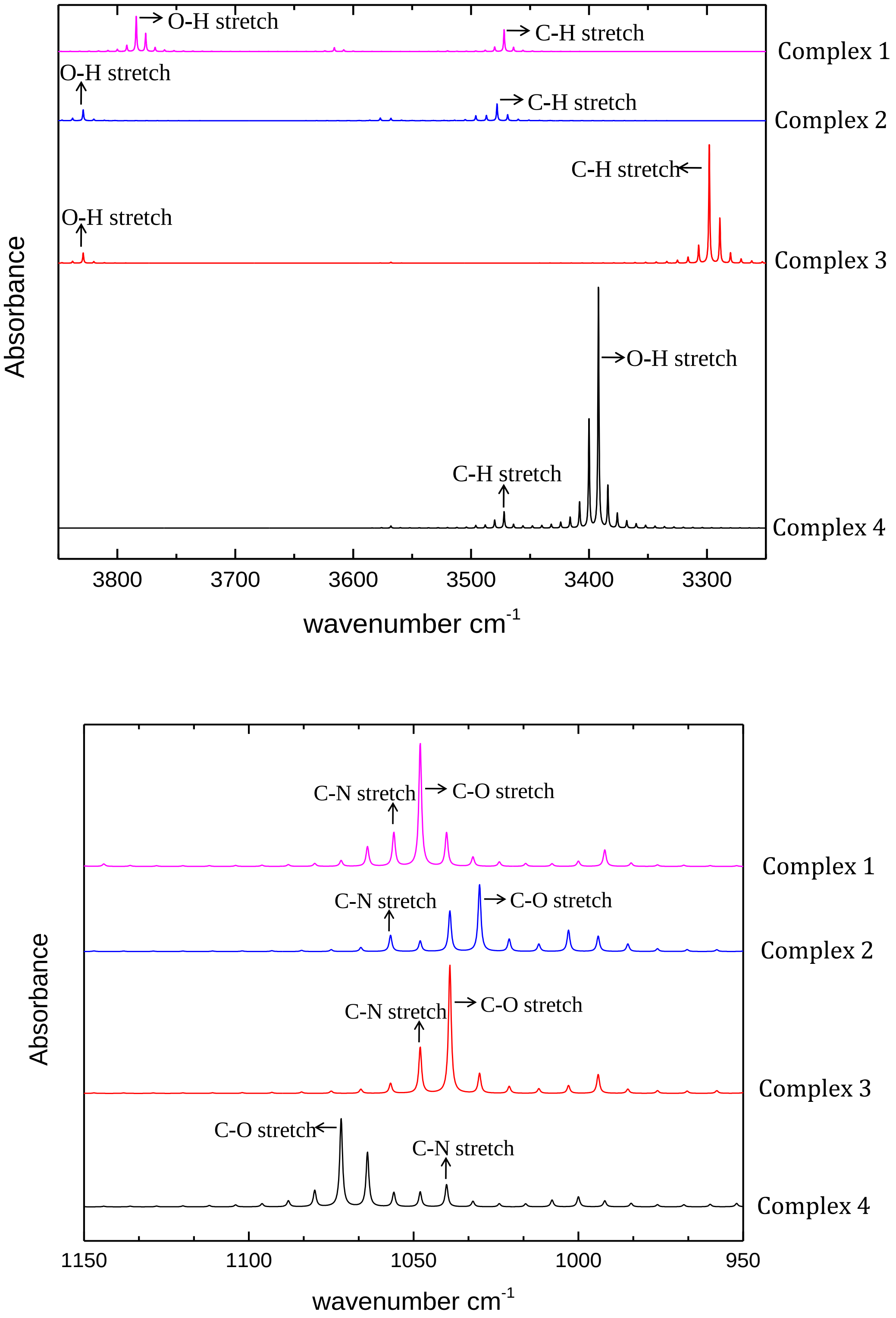

Figure 16: Computed spectra showing some of the important features in the propargyl alcohol-methyl amine complexes

AIM analysis

The charge density topology was studied by applying the atoms-in-molecules (AIM) theory by Bader to the optimized geometries. The method is based on analysis of electron density topology. Using the theory bond critical points (3, -1) and ring critical points (3, +1) associated with the complexes were located. Also, electron density $\rho(rc)$ and Laplacian of electron density $\nabla^2\rho(rc)$ were computed for the critical points, whose values are shown in Table 3. Large value of electron density for a critical point indicates the strength of the non covalent interaction present at the corresponding sites in the complexes. The structures obtained from AIM analysis which depict the critical points are shown in figure 17.

The existence and nature of hydrogen bond can be identified from Koch and Popelier criterion. This criterion characterizes the strength of the hydrogen bond depending on the electron density $\rho(rc)$ and Laplacian of electron density $\nabla^2\rho(rc)$ values as mentioned below.

1. $\nabla^2\rho < 0$ and $H < 0$ for strong H-bond of covalent nature
2. $\nabla^2\rho > 0$ and $H < 0$ for medium H-bond of partially covalent nature
3. $\nabla^2\rho > 0$ and $H > 0$ for weak H-bond of electrostatic character

where H is the total electron energy density at the bond critical point of interaction atoms.

It is therefore clear that our AIMS calculations indicate that the most stable complex, i.e. complex 4 with oxygen of propargyl alcohol as proton donor and the nitrogen of methyl amine as proton acceptor belongs to the category of a strong H-bond. Similar is the case with complex 1 and 2; while complex 3, where acetylene hydrogen is bonded with nitrogen of methyl amine, is indicated to a weak H-bond interaction.

Table 3: AIM calculations for the complexes obtained at B3LYP/6-311G++(d,p)

Complex	$\rho(rc)$ in e/(bohr)^3	$\nabla^2\rho(rc)$ in e/(bohr)^5
Complex 1	0.00448	-0.00440
Complex 2	0.00982	-0.01195
Complex 3	0.15430	0.01950
Complex 4	0.00791	-0.00817

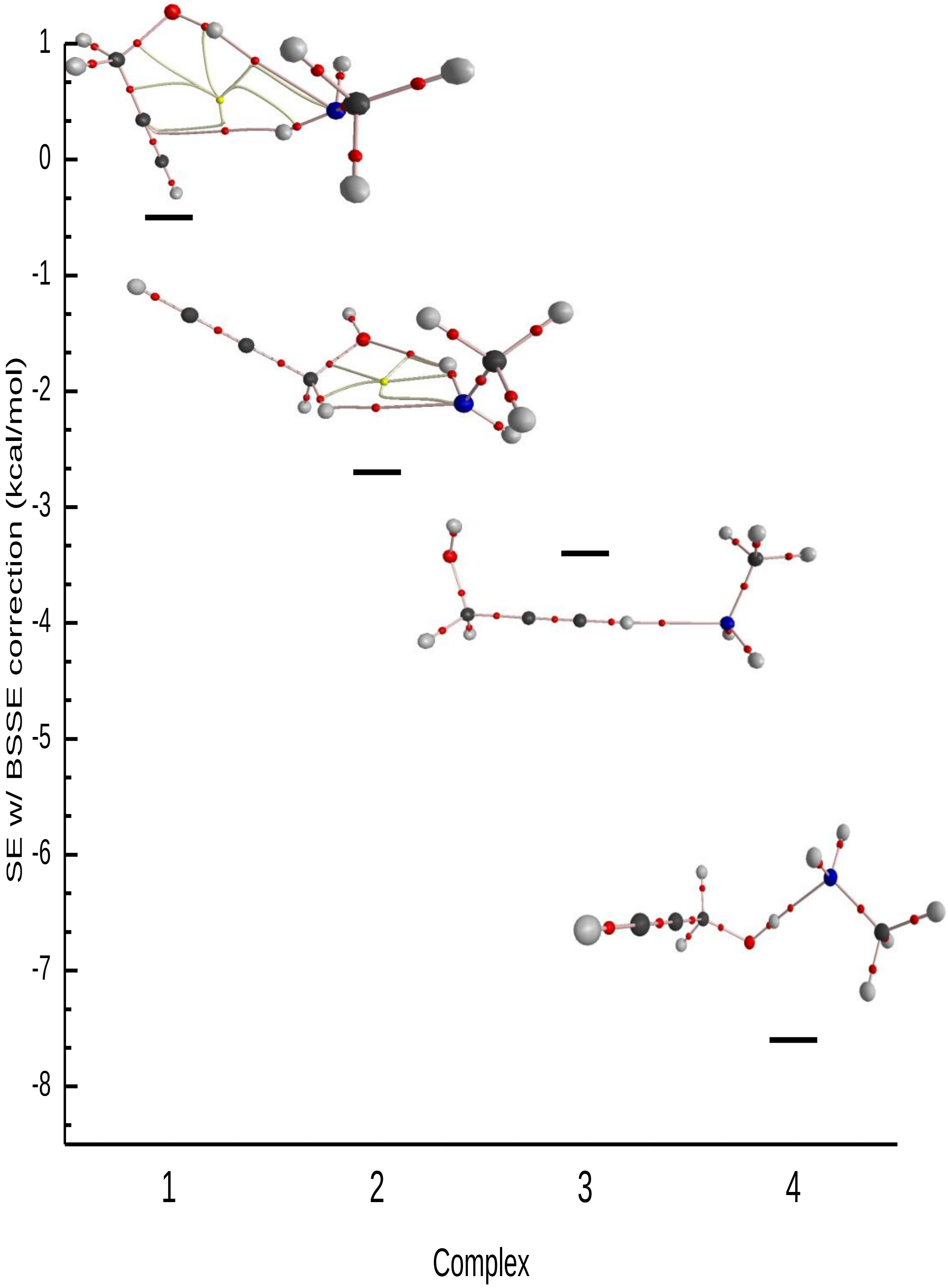

Figure 17: Structures of the complex showing the critical points obtained at the B3LYP /6-311++G(d,p)

3.3 RESULTS AND DISCUSSIONS

3.3.1 The individual features

The O-H stretch, acetylene C-H stretch, C-O stretch, and acetylene C-H bends of the propargyl alcohol were identified at 3642, 3310, 1040, 670 and 644 cm^{-1} respectively. These vibrations along with their computed values and scaling factors are listed in Table 4. Peaks at 3478 and 3458 cm^{-1} are assigned to the acetylene C-H stretches in propargyl alcohol dimer.[21.]

Table 4: Experimental frequencies and scaling factor of strong modes of propargyl alcohol

Mode of vibration	Experimental frequency cm^{-1}	Calculated frequency cm^{-1}	Scaling factor
O-H stretch	3642	3828.44	0.9513
acetylene C-H stretch	3310	3474.39	0.9527
C-O stretch	1040	1044.56	0.9963
acetylene C-H ⊥ bend	670	708.65	0.9454
acetylene C-H ‖ bend	644	664.34	0.9694

Features obtained in the methyl amine experiments were assigned by comparing them to the features mentioned in the work by Purnell et. al.[22.] These are shown in Table 5 with their computed values and scaling factors.

Table 5: Experimental frequencies and scaling factor of strong modes of methyl amine

Mode of vibration	Experimental frequency cm^{-1}	Calculated frequency cm^{-1}	Scaling factor
C-H a-sym stretch	2986	3092.00	0.9654
C-H a-sym stretch	2963	3056.15	0.9695
C-H sym stretch	2816	2961.52	0.9509
C-N stretch	1050	1055.92	0.9943
NH_2 wag	816	823.44	0.9910
CH_3 deform overtone*	2957		
CH_3 anti-sym + sym combination*	2933		
CH_3 anti-sym overtone*	2896		
CH_3 sym overtone*	2875		

*reference 21

3.3.2 The complex features

The features seen only in presence of both the molecules were compared with the computed frequencies of all the four complexes and assigned to the complex with the closest value (Table 6). In other words, the feature was attributed to the complex that had the least shift in the scaled frequency value from the experimental frequency of that feature.

Table 6: Frequency comparison and assignments for propargyl alcohol with methyl amine complexes

Experimental frequency	Scaled frequency of C1	Scaled frequency of C2	Scaled frequency of C3	Scaled frequency of C4	Assignment of mode of vibration
3191	3308 (117)	3311 (120)	3140 (-51)	3229 (38)	O-H stretch of PA in C4
3163	3308 (145)	3311 (148)	3140 (-23)	3229 (66)	acetylene C-H stretch of PA in C3
2861	2807 (-54)	2816 (-45)	2838 (-23)	2853 (-8)	C-H sym stretch of MA in C4
2854	2807 (-47)	2816 (-38)	2838 (-16)	2851 (-3)	C-H sym stretch of PA in C4
2843	2807 (-36)	2816 (-27)	2838 (-5)	2851 (8)	C-H sym stretch of PA in C3
1057	1043 (-14)	1030 (-27)	1036 (-21)	1065 (8)	C-O stretch of PA in C4
1036$^{\#}$	1043 (7)	1030 (-6)	1036 (0)	1037 (1)	C-N stretch of MA in C4
1034$^{\#}$	1043 (9)	1030 (-4)	1036 (2)	1037 (3)	C-O stretch of PA in C3
917$^{\#}$	904 (-13)	907 (-10)	914 (-3)	908 (-9)	NH_2 wag of MA in C4
911$^{\#}$	904 (-7)	907 (-4)	914 (3)	908 (-3)	acetylene C-H bend + NH_2 wag in C3
846		862 (16)	847 (1)	832 (-14)	acetylene C-H bend + NH_2 wag in C3
663	647 (-16)	644 (-19)		654 (-9)	acetylene C-H ⊥ bend in C4
632	647 (15)	644 (12)		632 (0)	acetylene C-H ‖ bend in C4

\# assignments based on intensity comparison

From Table 6 we see that complex 3 (C3) and complex 4 (C4) are identified. The feature at 3191 cm^{-1}, assigned to the shift in O-H frequency to C4, has a shift of 38 cm^{-1} from its scaled frequency; which is large. Anharmonic frequency calculation was also run for complexes 1-4 to check the contribution of anharmonicity to the observed shift in the vibrational features. It turned out that the effects of anharmonicity were negligible. The 3191 cm^{-1} feature was assigned to complex 4 as it appeared whenever the feature at 1057 cm^{-1} appeared, which was assigned to C4. The 1057 cm^{-1} feature is a blue shift from the features C-O stretch of propargyl alcohol and C-N stretch of methyl amine. Computationally, O-H stretch of propargyl alcohol in complex 4 is the only feature that shows a blue shift from the frequency of mode of vibration for the monomers. Furthermore, 1057 cm^{-1} feature is always accompanied by a small feature at 1036 cm^{-1}.

3.4 COMPLEXES WITH WATER

There are a few features in our co-deposition experiments which could not be assigned to the complexes of propargyl alcohol with methyl amine. Water being a ubiquitous impurity, the complexes of methyl amine with water and that of propargyl alcohol with water could not be ruled out. The complexes of propargyl alcohol with water, has already been studied in our laboratory [21]. The assignments of the propargyl-water complexes are shown in figure 18.

As mentioned earlier, complexes of methyl amine and water would be present even in experiments where no water was deliberately added. In order to confirm the features of the methyl amine-water complex, experiments were performed where water was deliberately added to methyl amine during deposition. The features that increased in intensity on increasing water concentration were studied; which are shown in figure 19.

Gaussian calculations were carried out to get optimized structures for methyl amine with water complexes using B3LYP with 6-311++G(d,p) basis set. In addition to exploring the presence of the 1:1 complexes of methyl amine-water, we also considered the possibility of observing the 1:2 complexes. Gaussian computations were performed and the structures are shown in figure 20. The vibrational frequencies of the higher complexes were also computed. Table 7 gives the stabilization energy of the 1:1 and 1:2 complexes. It can be seen that the stabilization energy of 1:2 adduct is more than twice the stabilization energy of 1:1 adduct; signifying that the interaction with a second molecule of water is favored by the first interaction. The frequencies were compared and the features were assigned; as shown in Table 8.

The structures obtained on AIM analysis of these structures to find critical points are shown in figure 21 and the charge density ρ and Laplacian of charge density $\nabla^2\rho$ values obtained in Table 9.

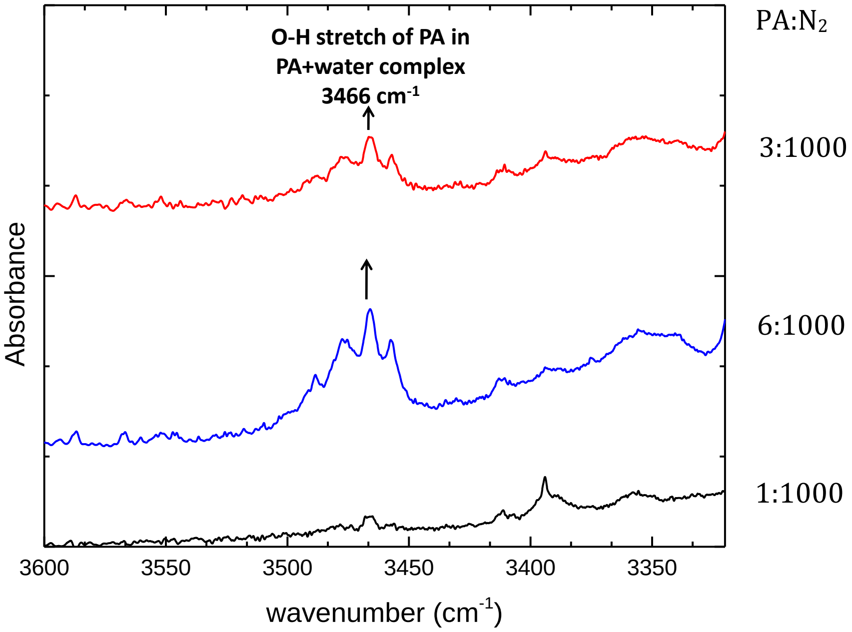

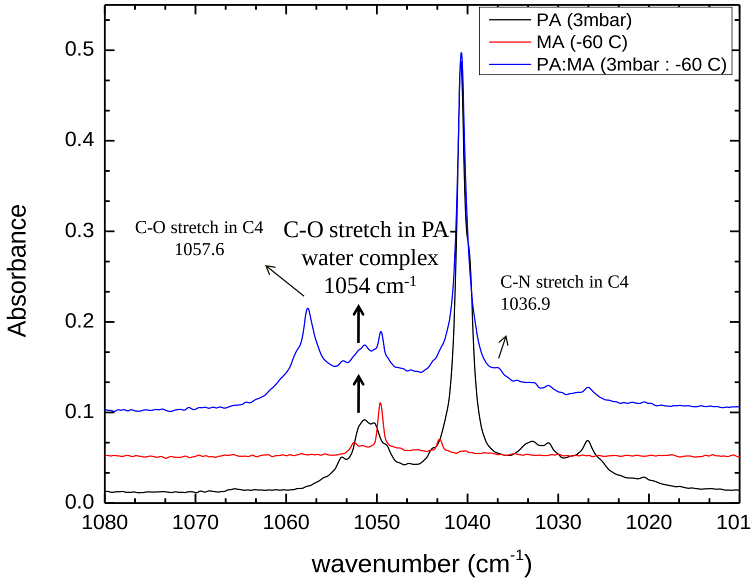

Figure 18: Spectral feature of propargyl alcohol and water complex in N_2 matrix

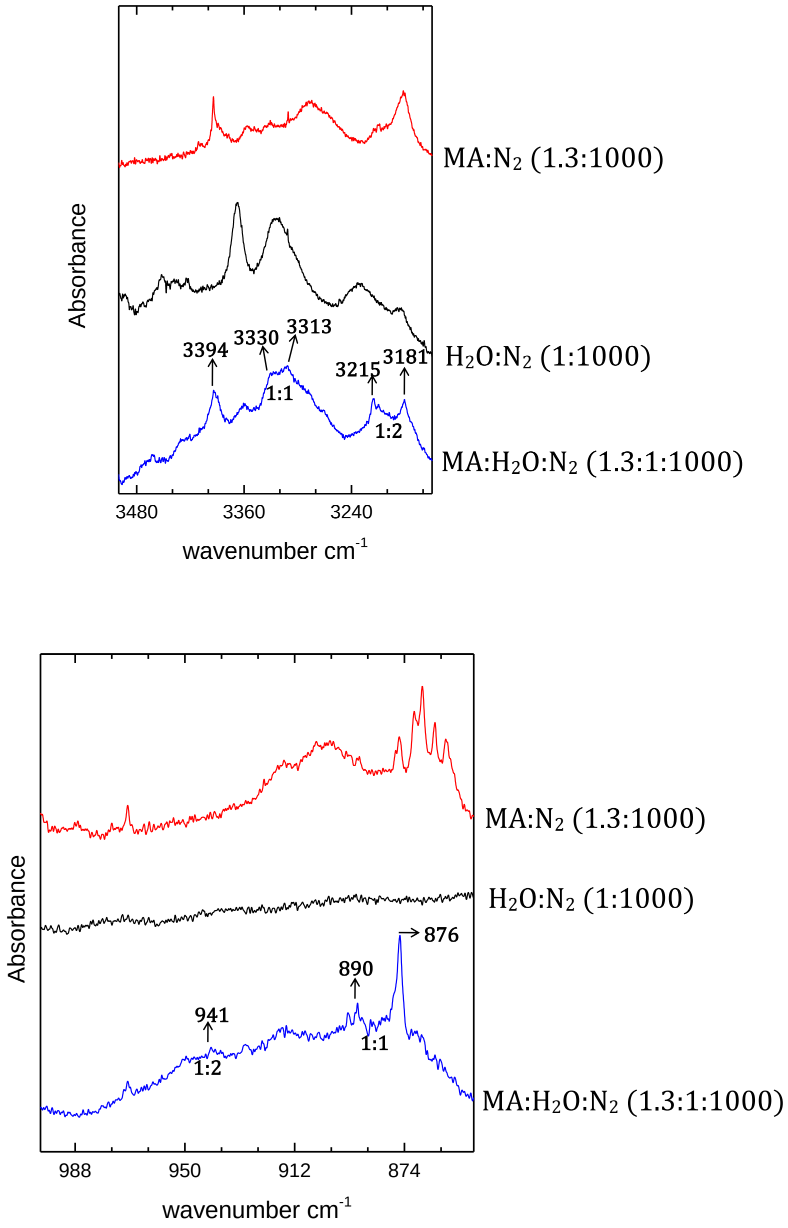

Figure 19: Features that are seen anew or that rise in intensity on deliberately adding water to methyl amine in N_2 matrix with $MA:H_2O:N_2$ – 1.3:1:1000

Table 7: Stabilization energies at B3LYP using 6-311++G(d, p) for MA-water complexes

Complex	**MA:water**	**ΔE_{Raw} , ΔE_{ZPE} , ΔE_{BSSE} (kcal/mol)**
MA-water	1:1	-7.6, -5.4, -6.9
MA-2 water	1:2	-17.1, -12.4, -15.5

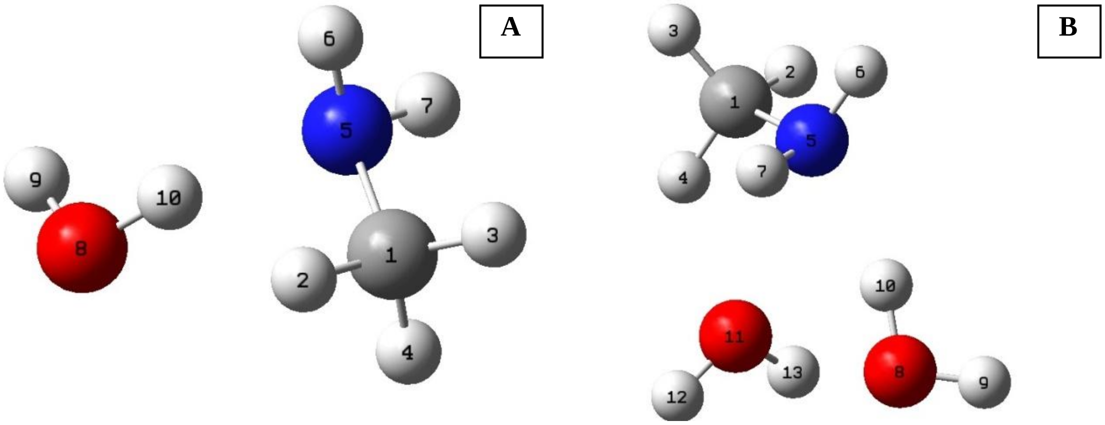

Figure 20: Optimized geometry structures obtained at B3LYP using 6-311++G(d, p) with their stabilization energies for methyl amine with water complexes A) 1:1 adduct B) 1:2 adduct

Table 8: Frequency comparison and assignments for methyl amine with water complexes

Experimental frequency	Scaled frequency of 1:1 adduct (A)	Scaled frequency of 1:2 adduct (B)	Assignment of mode of vibration
3330	3334 (4)	3410 (80)	bound O-H stretch of water + N-H stretch of MA in A
3313	3317 (4)	3282 (-31)	bound O-H stretch of water + N-H stretch of MA in A
3215	3004 (211)	3282 (67)	N-H sym stretch of MA in B
3181	3004 (-177)	3132 (-49)	O-H stretch of water in B
941	895 (-46)	953 (12)	CH_3 wag + NH_2 wag + bound OH wag combination in B
890	895 (5)	840 (-50)	CH_3 wag + NH_2 wag combination in A
876		840 (-36)	CH_3 wag + NH_2 wag + bound OH wag combination in B

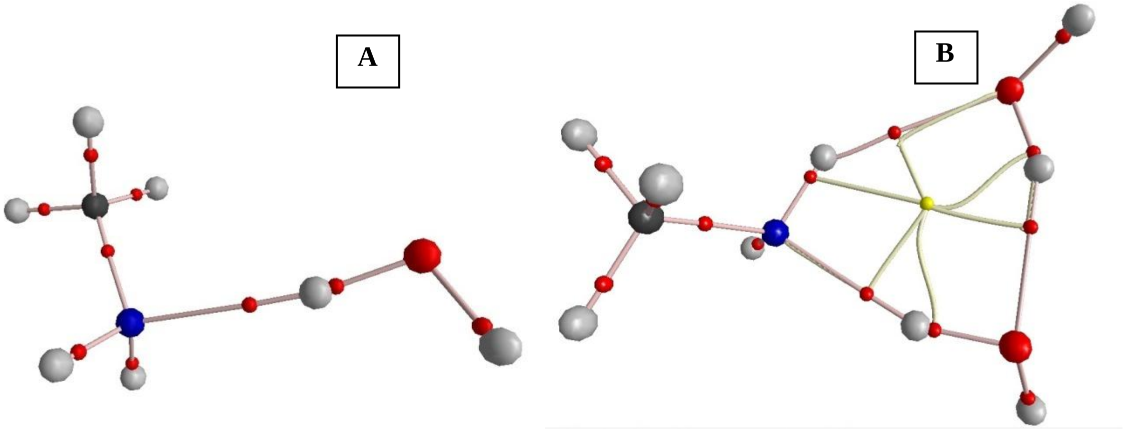

Figure 21: Structures of the complex showing the critical points obtained at the B3LYP /6-311++G(d,p)

Table 9: AIM calculations for the complexes obtained at B3LYP/6-311++G(d,p)

MA:water Complex	ρ(rc) in e/(bohr)^3	$\nabla^2\rho$(rc) in e/(bohr)^5
1:1	0.05162	-0.03414
1:2	0.02332	-0.02263

Chapter 4: Conclusions

Complexes of propargyl alcohol with methyl amine were studied by trapping the precursors in Ar and N_2matrices. The product bands of the 1:1 propargyl alcohol and methyl amine complexes were observed corresponding to a complex in which the hydrogen of the hydroxyl group of propargyl alcohol was hydrogen bonded to the nitrogen on methyl amine. This complex was also indicated to be the global minimum in our computations. Computations were done at the B3LYP/6-311++G**, MP2/6-311++G** and M06-2x/6-311++G** levels of theory. These levels of theory indicated four complexes as minima on the potential surface, with the global minimum being the structure described above and which was observed experimentally. In addition to the global minimum, a local minimum in which the acetylenic hydrogen of propargyl alcohol was bonded to the nitrogen of methyl amine was also observed. The experimental observations were corroborated by our computations. AIMs analysis was also done to establish the presence of hydrogen bonding in these structures. The values of ρ and the Laplacian at the bond-critical points of the hydrogen bond were in keeping with the values indicated by Koch and Popelier.

In addition to the above complex, we also studied the complexes of methyl amine and water. 1:1 complex of the two precursors were observed in our experiments, through a shift in the anti-symmetric stretch of the water sub-molecule. The observed shifts were corroborated by computations performed at the levels of theory indicated above for the propargyl alcohol/methyl amine. In addition, to the 1:1 complex, we also observed 1:2 methyl amine-water complex in our matrix. Computations were also performed to confirm the presence of this complex. AIMS analysis was also performed to understand the nature of the hydrogen bonded interactions in these systems.

Bibliography

1. M. J. S. Dewar, *J. Chem. Soc*. **1944**, 406
2. G. A. Jeffrey and W. Saenger, Hydrogen Bonding in Biology and Chemistry, Springer-Verlag, Berlin, **1991**
3. JiHye Lee, et al. *Phys. Chem. A*, **2010, 5,** 114
4. Yunju Zhang, et. al. *J. Comp. Chem*. **2014**, 35, 1646–1656
5. H. E. Hallam, Vibrational Spectroscopy of Trapped Species, John Wiley and Sons, London, **1973**
6. G. C. Pimentel, S. W. Charles, *Pure and Appl. Chem*., **1963**, 7, 111
7. www.arscryo.com/TechNotes
8. www.globalspec.com/learnmore
9. S. Cradock, A. J. Hinchcliffe, Matrix Isolation, Cambridge University Press,**1975**
10. A. D. Becke, *Phys. Rev. A*, **1989**, 38, 3098
11. A. D. Becke, *J. Chem. Phys*., **1983**, 98, 5648
12. C. Lee, N. Yang, R. G. Parr, *Phys. Rev. B*, **1988**, 37, 785
13. S. F. Boys, F. Bernadi, *Mol. Phys*., **1970**, 19, 553
14. F. Jensen, *Chem. Phys. Lett*., **1996**, 261, 633
15. I. Mayer, P. R. Surján, *Chem. Phys. Lett*., **1992**, 191, 497
16. D. W. Schwenke, D. G. Truhlar, *J. Chem. Phys*., **1985**, 82, 24184
17. L. Turi, J. J. Dannenberg, *J. Phys. Chem*., **1993**, 97, 2488
18. L. Turi, J. J. Dannenberg, *J. Phys. Chem*., **1995**, 99, 639
19. N-B. Wong, Y-S. Cheung, D. Y. Wu, Y. Ren, X. Wang, A. M. Tian, W-K. Li, *J. Mol. Struct*., **2000**, 507, 153
20. M. J. Frisch, G. W. Trucks, H. B. Schlegel, P. M. W. Gill, B. G. Johnson, M. A. Robb, J.R. Cheeseman, T. Keith, G. A. Peterson, J. A. Montgomery, K. Raghavachari, M. A. Al-laham, V. G. Zakrzewski, J. V. Ortiz, J. B. Foresman, J. Cioslowski, B. B. Stefanov, A.Nanayakkara, M. Challacombe, C. Y. Peng, P. Y. Ayala, W. Chen, M. W. Wong, J. L.Andres, E. S. Replogle, R. Gomperts, R. L. Martin, D. J. Fox, J. S. Binkley, D. J. Defrees, J. Baker, J. P. Stewart, M. Head- Gordon, C. Gonzalez, J. A. Pople, GAUSSIAN 09, Revision D.1,Gaussian Inc., Pittsburgh, PA, **1995**
21. J. Saini, MS Thesis report, IISER Mohali, **2014**
22. C. J. Purnell, *Chem. Phys*., **1976**, 12, 77-87

23. D. Trogoloet. al., *J. Phys. Chem*. A **2013**, 427-440
24. www.astrochymist.org
25. B. T. Mmereki and D. J. Donaldson, *J. Phys. Chem*. A **2002**, 106, 3185-3190
26. www.unmannedspaceflight.com